
Article:
Tan, C.H., Velichko, A., Lim, L.W. et al. (1 more author) (2019) Few-photon detection using InAs avalanche photodiodes. Optics Express, 27 (4). pp. 5835-5842. ISSN 1094-4087

https://doi.org/10.1364/OE.27.005835

Research Article | Vol. 27, No. 4 | 18 Feb 2019 | OPTICS EXPRESS 5835
Optics EXPRESS

Few-photon detection using InAs avalanche photodiodes

CHEE HING TAN,* ANTON VELICHKO, LEH WOON LIM, AND JO SHIEN NG

Department of Electronic and Electrical Engineering, University of Sheffield, Sheffield S3 7HQ, UK
**c.h.tan@sheffield.ac.uk*

Abstract: An avalanche photodiode with a ratio of hole-to-electron ionization coefficients, $k = 0$, is known to produce negligible excess noise irrespective of the avalanche gain. The low noise amplification process can be utilized to detect very low light levels. In this work, we demonstrated InAs avalanche photodiodes with high external quantum efficiency of 60% (achieved without antireflection coating) at the peak wavelength of 3.48 µm. At 77 K, our InAs avalanche photodiodes show low dark current (limited by 300 K blackbody background radiation), high avalanche gain and negligible excess noise, as InAs exhibits $k = 0$. They were therefore able to detect very low levels of light, at 15-31 photons per 50 µs laser pulse at 1550 nm wavelength. These correspond to the lowest detected average power by InAs avalanche photodiodes, ranging from 19 to 40 fW. The measurement system's noise floor was dominated by the pre-amplifier. Our results suggest that, with a lower system noise, InAs avalanche photodiodes have high potential for optical detection of single or few-photon signal levels at wavelengths of 1550 nm or longer.

1. Introduction

The ability to detect light efficiently is increasingly important for applications in communications, security, medicine and metrology. Conventional semiconductor photodiodes have limited sensitivity, especially in photon-starved and high-speed applications such as free space optical communication and remote sensing. In these applications, avalanche photodiodes (APDs) are often the preferred optical detectors. APDs utilize their internal gain, achieved via impact ionization, to transform electron-hole pairs generated by a few absorbed photons into an avalanche of charged carriers, resulting in a much larger, detectable electrical signal.

Two key performance parameters in conventional APDs are the mean gain, M, and the excess noise factor, F. The latter characterizes the additional noise caused by the impact ionization process. It is known that an avalanche material with disparate electron and hole ionization coefficients, α and β, respectively, exhibits low excess noise factors [1], provided the carrier with the higher ionization coefficient initiates the avalanche process. Assuming insignificant dead spaces and uniform electric field, $F = kM + (1-k)(2 - 1/M)$, where $k = \beta/\alpha$ (or α/β) for an electron (or a hole) initiated avalanche process [1]. In an ideal APD, the minimum excess noise factor limit of 2 is obtained at large M, when $\beta = 0$, i.e. $k = 0$ (for $\alpha > \beta$ and electron-initiated avalanche process). Thus a non-zero k limits the maximum gain from an APD before its excess noise degrades its performance.

Among the well-characterized semiconductor materials, Si APDs exhibit k between 0.05 and 0.1, for APD designs with thick avalanche regions (operating voltages > 100 V) [2] and those with thin avalanche regions (operating voltages ~30-40 V) [3]. Consequently Si APDs dominate light sensing applications at operating wavelengths, λ, between 0.4 and 1.0 µm. For the shortwave infrared (IR) light with λ between 1.0 and 1.6 µm, InGaAs/InP APDs (originally developed for optical fiber communication systems) are currently the most

#340662 https://doi.org/10.1364/OE.27.005835
Journal © 2019 Received 26 Jul 2018; revised 19 Dec 2018; accepted 26 Dec 2018; published 15 Feb 2019

Optics EXPRESS

commonly used APDs. They typically exhibit k ~0.4, higher than the more recently developed InGaAs/InAlAs APDs (k ~0.2 [4]).

Unlike APDs for optical fiber communications, low photon or single photon detection demands APDs operating with gains in excess of 10^4 in tandem with a low noise pre-amplifier. At such a high gain, achieving $F \rightarrow 1$, below the conventional excess noise theory is desirable. Over the past two decades, several ideas have been proposed to reduce k to realize low-noise shortwave IR APDs. These include APDs incorporating avalanche region consisting staircase band-structures [5,6], superlattices [7], impact-ionization-engineered heterojunctions [8], Si (with fused InGaAs absorption region) [9], Si (with Ge absorption region) [10] and more recently AlGaAsSb [11] and AlInAsSb [12]. Of these, the most promising APDs are those incorporating Si, AlGaAsSb and AlInAsSb avalanche regions, because they exhibit low noise, k ~0.01-0.1. More commonly, APDs currently used for very low photon detection are those designed to operate in 'Geiger' mode, in which the APD is biased beyond its breakdown voltage.

In a Geiger mode APD, absorption of a single photon can result in a large current pulse so the device is also called Single Photon Avalanche Diode (SPAD). Commercial Si-based SPADs, produced by custom processes [13] or CMOS technologies [14], can detect single photons with wavelengths of 0.4-1.0 μm. Typical values for peak single photon detection efficiency (SPDE) of Si-based SPADs are 40-50%, usually occurring at 400-500 nm wavelength. Improved CMOS processes and designs have improved the peak SPDE, although SPDE at longer wavelengths remain low. For example, the red-enhanced SPAD reported in [15] exhibited SPDE of 60, 12, and 1% at wavelength of 500, 800 and 1000 nm, respectively.

For detecting photons with wavelengths between 1.0 and 1.6 μm, commercially available InGaAs/InP SPADs [16] offer typical SPDE up to 32% at 1550 nm wavelength. Higher SPDE (exceeding 55% at 1550 nm) was achieved by incorporating more effective cancellations of capacitive transient in InGaAs/InP SPADs [17]. Alternatively, Superconducting Nanowire Single Photon Detectors (SNSPDs) offer much higher SPDE (typically > 80%), but with the significant disadvantage of cryogenic cooling down to ~2 K. Since such cooling requirement is incompatible with practical, large-scale adoption of quantum communication (optical fiber-based [18] or air-ground [19]) and quantum imaging [20,21], high performance SPADs for wavelengths of 1.0-1.6 μm are highly desirable.

An avalanche material with $F \rightarrow 1$ would be ideal for single photon detection. It can offer photomultiplier-like characteristics, such as high gain with negligible amplification noise and very fast detection, as well as enable photon number analysis. Avalanche materials exhibiting F ~1.0-1.5, such as InAs [22] and HgCdTe [23–25], also have high quantum efficiency and are suitable for imaging arrays, making them potentially the most desirable type of single photon detector in the mid infrared range. The excess noise factor below 2 can be explained by the dead space effects [26], when the dead space is comparable to the mean distance between impact ionization.

Single photon detection using HgCdTe APDs [27] and small-format APD arrays [28] have been reported. In [28], the 4x4 array cooled to 77 K was able to detect optical pulses as weak as 1 or 20 photons per pulse for pulse width of 70 ps or 1 μs, respectively. Despite excellent performance from HgCdTe APDs, an alternative detector technology such as InAs APDs for operation at and beyond 1550 nm wavelength is worthwhile because HgCdTe APDs are both expensive and incompatible with the global initiative to eventually phase out the use of mercury [29]. In this work, we report the performance of InAs APDs in detecting very weak optical pulses at 1550 nm wavelength. The lower detection limit, currently imposed by electronic noise, was found to be ~15 photons within a 50 μs pulse.

Optics EXPRESS

2. Experimental details

The InAs APDs used in this work were fabricated from a wafer grown by molecular beam epitaxy on a (100) n-type InAs substrate. The wafer structure details are shown schematically in Fig. 1(a). The wafer includes a highly doped 100 nm p-type InAs layer for low ohmic resistance. This is followed by a layer of $AlAs_{0.16}Sb_{0.84}$, which presents a large conduction band barrier of ~1.22 eV [30], to reduce undesirable diffusion of minority electrons from the surface. We have made two changes to our APDs relative to our previous generation of InAs APDs [31]. A relatively thick InAs p-type absorption layer of 3500 nm (compared to 700 nm in [31]) ensures pure electron injection at the intended wavelength of operation, 1550 nm. A linearly graded p-type doping profile in this p-layer reduces loss of photogenerated electrons through recombination with the majority holes. To achieve higher avalanche gain, the avalanche region consists of a 6000 nm (compared to 3500nm in [31]) thick unintentionally doped InAs layer.

Using device fabrication procedures described in [32], mesa APDs with optical windows and nominal diameters of 240 μm were produced. No antireflection coating was deposited on the optical window. An APD under test is shown with probe tips in contact with its metal contacts and optical fiber's end over its optical window in Fig. 1(b).

Measurements were carried out on the InAs APDs to obtain the dark current versus voltage characteristics (forward and reverse bias), responsivity versus wavelength at a fixed reverse bias, avalanche gain versus reverse bias, and weak light detection. For all measurements, the device-under-test (DUT) was placed in a low temperature probe station (model ST-500 of Janis Research), which maintained the desired temperature of the DUT ranging from 77 and 300 K. The probe station coupled external light into the device chamber with an optical fiber feed-through connected to micromanipulators.

For the spectral response measurements, a monochromator-tungsten lamp combination provided monochromatic light at wavelength from 600 to 4000 nm, to facilitate measurements of photocurrent versus wavelength on our InAs APDs and a reference diode (Judson J12-18C-250U).

For the avalanche gain measurements, the light source was a 1550 nm wavelength laser modulated at 10 kHz with 50% duty cycle ratio. The optical path included two fixed optical attenuators (26.5 dB each) and a calibrated variable optical attenuator (0-80 dB) to obtain the required optical attenuation. The DUT's photocurrent was amplified and converted into a voltage signal by a low-noise current preamplifier (model SR570 of Stanford Research Systems), before being measured by a lock-in amplifier. The avalanche gain was defined as the ratio of the photocurrent measured using a lock-in amplifier to the unity gain photocurrent at V_r = -1.0 V.

The measurements for weak light detection used an identical setup as the avalanche gain measurements, except that the lock-in amplifier was replaced with a spectrum analyzer (model SR760 of Stanford Research Systems). This was chosen to clearly illustrate the signal and noise levels during the measurements.

Optics EXPRESS

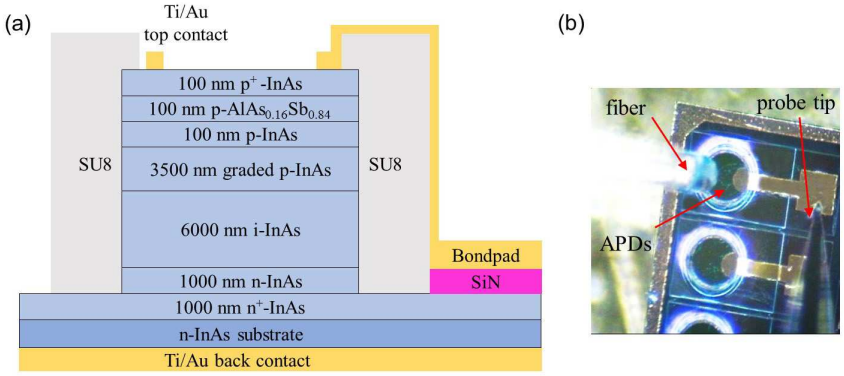

Fig. 1. (a) Cross-sectional schematic diagram of InAs APD. (b) Fabricated APDs with diameters of 240 μm.

3. Results

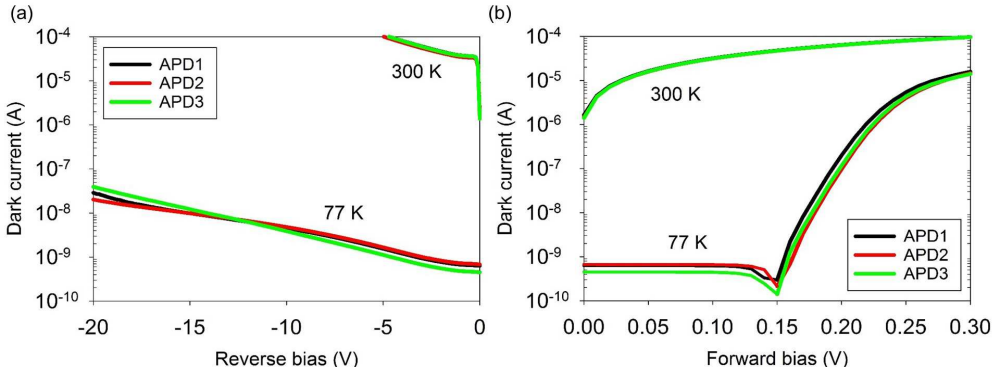

Fig. 2. Data of dark current versus voltage in (a) reverse and (b) forward bias at 300 and 77 K.

A total of 10 devices were tested. Only results from 3 of the best APDs, referred to as APD1, APD2 and APD3, are presented for clarity. Dark current versus voltage characteristics of the InAs APDs at 77 and 300 K are shown in Fig. 2. Three sets of data are shown for a given set of experimental conditions and they are in agreement. In the forward bias shown in Fig. 2(b), the dark current drops rapidly when the APDs were cooled from 300 to 77 K. At 77 K, the dark currents at forward bias voltages from 0 to 0.13 V are fairly constant and range between 450 and 670 pA, demonstrating a photovoltaic effect with a clear increase in the open-circuit voltage. This constant current extends to the reverse bias voltages in Fig. 2(a), V_r, of 0 to −1.0 V. They are interpreted as background radiations from parts of the probe station chamber at higher temperatures than the DUT. Beyond −1.0 V, dark currents increase with reverse bias rapidly. Clearly the dark current could be reduced by reducing the device diameter to below 240 μm in future work.

Optics EXPRESS

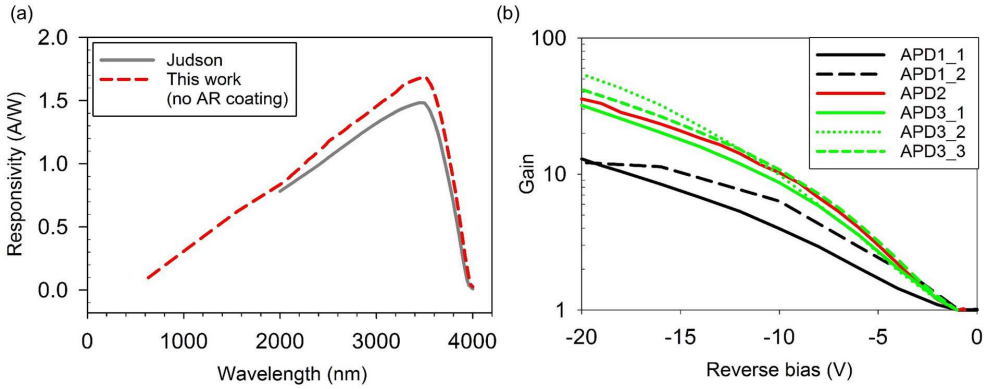

Fig. 3. (a) Measured room temperature responsivity from our InAs APDs reverse-biased at –0.2 V. Data for a commercial reference InAs photodiode are also included. (b) 77 K avalanche gain measured on three APDs using a 1550 nm laser.

Data of responsivity versus wavelength for our InAs APD at V_r = –0.2 V at 300 K are compared with those of the commercial reference InAs photodiode in Fig. 3(a). Note that there is no appreciable avalanche gain from the InAs APD at –0.2 V (see data later). At wavelengths between 2.0 and 4.0 μm, our InAs APDs exhibit higher responsivity than the commercial reference diode. Peak responsivity values are 1.68 and 1.48 A/W in our APD and the reference diode, respectively. Our measured peak responsivity of 1.68 A/W at the peak wavelength of 3.48 μm corresponds to an external quantum efficiency of 60%. Even higher responsivity may be obtained by including anti-reflection coating on our APDs to minimize light reflection at the air-semiconductor interface.

In Fig. 3(b), experimental avalanche gain versus reverse bias characteristics from three APDs (APD1, APD2 and APD3), repeated on different days (where possible), are compared. There are two and three sets of data for APD1 and APD3 respectively, but only a single set of data for APD2, which had degraded by the time a second measurement was attempted. For a given reverse bias, it can be observed that the avalanche gain varies between different APDs and different measurements for the same APD.

The variations observed in Fig. 3(b) are attributed to uncertainties in the position of the optical fiber's tip in relation to the optical window of the DUT. Different photocurrent readings (e.g. 7.1, 2.6, and 2.3 nA) from repeated measurements on a given DUT at –1.0 V were recorded, when the measurements involved optical fiber re-positioning. Much of the uncertainties associated with the positioning of the optical fiber stems from the optical fiber being transparent (as shown in Fig. 1(b)). It is possible that the 1550 nm wavelength light may have been injected at the sidewall of the mesa APDs, leading to different carrier generation profiles. Since electron ionization coefficients are much larger than hole ionization coefficients, mixed carrier injection produces lower gain than pure electron injection. Hence variation in the avalanche gain in Fig. 3(b) is believed to arise from different carrier generation profiles.

The three APDs were used in further photocurrent measurements for weak light detection. The 1550 nm wavelength light was heavily attenuated and the mean number of photons per pulse was estimated using the optical attenuation setting and responsivity value of 0.52 A/W. Spectra of power density versus frequency from APD3 at –6 and –18 V using optical signals with 391 or 196 photons per pulse are shown in Fig. 4.

As expected, a higher optical power leads to a stronger power density peak. For a given optical power, increasing the reverse bias increases the power density peak from the APD because of increasing avalanche gain. The data also show that the noise floor of the spectra is unaffected by the reverse bias applied to the DUT and the corresponding change in dark

Optics EXPRESS

current. Combining this with the pre-amplifier having a noise floor of 0.2 μV/Hz$^{1/2}$ at a gain of 10^5 V/A, we attribute the noise floor observed from Fig. 4 to the measurement system noise. In addition, it is expected that if the total current in our APD is << 1 μA, the resultant shot noise would remain insignificant compared to the pre-amplifier noise.

Data in Fig. 4 also indicate that avalanche gain does not contribute to significant noise. This is expected since InAs APDs exhibit excess noise factor of ~1.5 independent of gain and temperature [31]. Hence the APD's signal-to-noise ratio increases from 3 at −6 V to 24.45 at −18 V, for an optical power of 1 pW (391 photons over a 50 μs pulse) and assuming a noise floor of 0.2 μV/Hz$^{1/2}$.

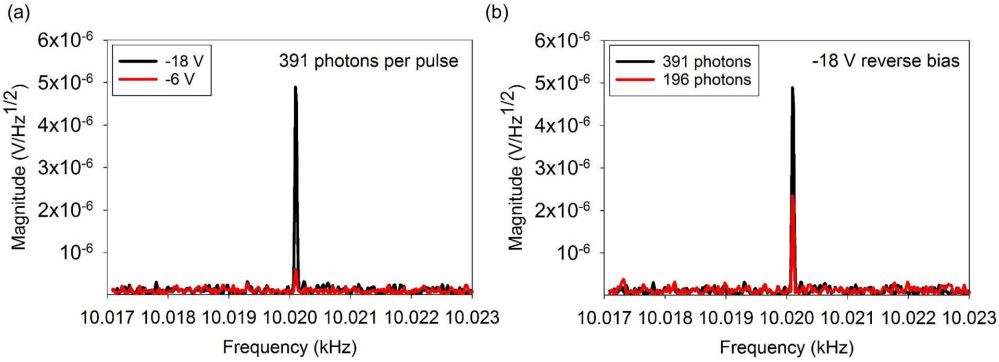

Fig. 4. Measured power spectrum density of APD3 at 77 K, at (a) different reverse bias voltages and (b) different photon numbers. These measurements were taken with a span of 6 Hz.

Having achieved a good signal-to-noise ratio, we further reduced the optical power to investigate the performance of our APDs under low photon conditions. Our best results are shown in Fig. 5. The noise floor is predominantly contributed by the system noise. However due to the differences in the avalanche gain we had to bias the APDs at different reverse biases to achieve the best SNR. Since the carrier generation profiles are different, the peak magnitude measured is different in each spectrum. The zoomed-in spectra taken using the SR760 spectrum analyzer with a span of 0.76 Hz show clear signal peaks corresponding to 15-31 photons per 50 μs laser pulse. The corresponding detected average power ranges from 19 to 40 fW, giving a signal-to-noise ratio above 2. Given the preamplifier noise is nominally specified to be 0.2 μV/Hz$^{1/2}$, a larger signal to noise ratio may be achieved if an amplifier with lower noise is used. Therefore with improved quantum efficiency (possibly via an optimized antireflection coating) and a lower amplifier noise, InAs avalanche photodiodes could detect single or few-photon signals at 1.55 μm or longer wavelengths (with high responsivity as shown in Fig. 3(a)), which are ideal for eye-safe imaging, range measurement and gas sensing applications.

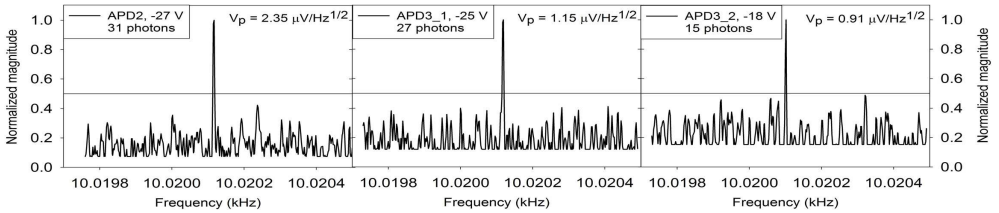

Fig. 5. Measured power spectrum density of APD2 and APD3 at 77 K. The peak magnitude corresponding to the number of absorbed photons is included at the top-right corner of each spectrum. These measurements were taken with a span of 0.76 Hz. The lines at 0.5 normalized magnitude were included to illustrate that signal to noise ratio is larger than 2.

Optics EXPRESS

4. Conclusion

InAs avalanche photodiodes have been fabricated and evaluated for low photon detection at a wavelength of 1.55 μm. A high external quantum efficiency of 60% at the peak wavelength of 3.48 μm was obtained (without antireflection coating) at room temperature. When cooled to 77 K, the dark current was found to be limited by 300 K background radiation. The high quantum efficiency, low dark current and negligible excess noise factor enable our InAs avalanche photodiodes to detect very low light levels of 15-31 photons per 50 μs laser pulse at a wavelength of 1.55 μm. The corresponding detected average power ranges from 19 to 40 fW. Measurements using the spectrum analyzer indicated that the noise floor is dominated by the pre-amplifier noise. These suggest that a fully optimized InAs avalanche photodiode (for example with an optimized antireflection coating) coupled to a pre-amplifier with lower noise can achieve single or few photon detection at 1.55 μm or longer wavelengths.

Funding

Engineering and Physical Sciences Research Council (EPSRC) (EP/H031464/1); European Space Agency (ESA) (4000107110/12/NL/CBi).

Acknowledgments

The data reported in this paper is available from the ORDA digital repository (DOI: 10.15131/shef.data.6859820).

References

1. R. J. McIntyre, "Multiplication noise in uniform avalanche diodes," IEEE Trans. Electron Dev. **ED-13**(1), 164–168 (1966).
2. H. Kanbe, T. Kimura, Y. Mizushima, and K. Kajiyama, "silicon avalanche photodiodes with low multiplication noise and high-speed response," IEEE Trans. Electron Dev. **23**(12), 1337–1343 (1976).
3. C. H. Tan, J. C. Clark, J. P. R. David, G. J. Rees, S. A. Plimmer, R. C. Tozer, D. C. Herbert, D. J. Robbins, W. Y. Leong, and J. Newey, "Avalanche noise measurement in thin Si p^+-i-n^+ diodes," Appl. Phys. Lett. **76**(26), 3926–3928 (2000).
4. Y. L. Goh, A. R. J. Marshall, D. J. Massey, J. S. Ng, C. H. Tan, M. Hopkinson, J. P. R. David, S. K. Jones, C. C. Button, and S. M. Pinches, "Excess avalanche noise in $In_{0.52}Al_{0.48}As$," IEEE J. Quantum Electron. **43**(6), 503–507 (2007).
5. G. F. Williams, F. Capasso, and W. T. Tsang, "The graded bandgap multilayer avalanche photodiode: a new low-noise detector," IEEE Electron Device Lett. **3**(3), 71–73 (1982).
6. M. Ren, S. Maddox, Y. Chen, M. Woodson, J. C. Campbell, and S. Bank, "AlInAsSb/GaSb staircase avalanche photodiode," Appl. Phys. Lett. **108**(8), 081101 (2016).
7. F. Capasso, W. T. Tsang, A. L. Hutchinson, and G. F. Williams, "Enhancement of electron impact ionization in a superlattice: A new avalanche photodiode with a large ionization rate ratio," Appl. Phys. Lett. **40**(1), 38–40 (1982).
8. P. Yuan, S. Wang, X. Sun, X. G. Zheng, A. L. Holmes, and J. C. Campbell, "Avalanche photodiodes with an impact-ionization-engineered multiplication region," IEEE Photonics Technol. Lett. **12**(10), 1370–1372 (2000).
9. Y. Kang, P. Mages, A. R. Clawson, P. K. L. Yu, M. Bitter, Z. Pan, A. Pauchard, S. Hummel, and Y. H. Lo, "Fused InGaAs-Si avalanche photodiodes with low-noise performances," IEEE Photonics Technol. Lett. **14**(11), 1593–1595 (2002).
10. Y. Kang, M. Zadka, S. Litski, G. Sarid, M. Morse, M. J. Paniccia, Y. H. Kuo, J. Bowers, A. Beling, H.-D. Liu, D. C. McIntosh, J. Campbell, and A. Pauchard, "Epitaxially-grown Ge/Si avalanche photodiodes for 1.3 μm light detection," Opt. Express **16**(13), 9365–9371 (2008).
11. L. L. G. Pinel, S. J. Dimler, X. Zhou, S. Abdullah, S. Zhang, C. H. Tan, and J. S. Ng, "Effects of carrier injection profile on low noise thin $Al_{0.85}Ga_{0.15}As_{0.56}Sb_{0.44}$ avalanche photodiodes," Opt. Express **26**(3), 3568–3576 (2018).
12. S. R. Bank, J. C. Campbell, S. J. Maddox, M. Ren, A. Rockwell, M. E. Woodson, and S. D. March, "Avalanche photodiode based on the AlInAsSb Materials System," IEEE J. Sel. Top. Quantum Electron. **24**(2), 3800407 (2018).
13. Micro Photon Devices, "PDM series photon counting detector modules datasheet" (Micro Photon Devices). http://www.micro-photon-devices.com/Docs/Datasheet/PDM.pdf. Accessed 25 April 2018.
14. Micro Photon Devices, "SPC2 series photon counting camera datasheet" (Micro Photon Devices). http://www.micro-photon-devices.com/Docs/Datasheet/SPC2.pdf. Accessed 25 April 2018.

Optics EXPRESS

15. M. Sanzaro, P. Gattari, F. Villa, A. Tosi, G. Croce, and F. Zappa, "Single-photon avalanche diodes in a 0.16 μm BCD technology with sharp timing response and red-enhanced sensitivity," IEEE J. Sel. Top. Quantum Electron. **24**(2), 1–9 (2018).
16. Micro Photon Devices, "InGaAs Single-Photon Counter" (Micro Photon Devices, 2014). http://www.micro-photon-devices.com/Docs/Datasheet/InGaAs_Datasheet.pdf. Accessed 27 April 2018.
17. L. C. Comandar, B. Fröhlich, J. F. Dynes, A. W. Sharpe, M. Lucamarini, Z. L. Yuan, R. V. Penty, and A. J. Shields, "Gigahertz-gated InGaAs/InP single-photon detector with detection efficiency exceeding 55% at 1550 nm," J. Appl. Phys. **117**(8), 083109 (2015).
18. B. Korzh, C. C. W. Lim, R. Houlmann, N. Gisin, M. J. Li, D. Nolan, B. Sanguinetti, R. Thew, and H. Zbinden, "Provably secure and practical quantum key distribution over 307 km of optical fibre," Nat. Photonics **9**(3), 163–168 (2015).
19. S. Nauerth, F. Moll, M. Rau, C. Fuchs, J. Horwath, S. Frick, and H. Weinfurter, "Air-to-ground quantum communication," Nat. Photonics **7**(5), 382–386 (2013).
20. D. S. Simon, G. Jaeger, and A. V. Sergienko, *Quantum Metrology, Imaging, and Communication*, (Springer International Publishing, 2017).
21. M. Buttafava, J. Zeman, A. Tosi, K. Eliceiri, and A. Velten, "Non-line-of-sight imaging using a time-gated single photon avalanche diode," Opt. Express **23**(16), 20997–21011 (2015).
22. A. R. J. Marshall, C. H. Tan, M. J. Steer, and J. P. R. David, "Extremely low excess noise in InAs electron avalanche photodiodes," IEEE Photonics Technol. Lett. **21**(13), 866–868 (2009).
23. I. M. Baker, S. S. Duncan, and J. W. Copley, "A low-noise laser-gated imaging system for long-range target identification," Proc. SPIE **5406**, 133–144 (2004).
24. J. Beck, C. Wan, M. Kinch, J. Robinson, P. Mitra, R. Scritchfield, F. Ma, and J. Campbell, "The HgCdTe electron avalanche photodiode," J. Electron. Mater. **35**(6), 1166–1173 (2006).
25. J. Rothman, L. Mollard, S. Bosson, G. Vojetta, K. Foubert, S. Gatti, G. Bonnouvrier, F. Salveti, A. Kerlain, and O. Pacaud, "Short-wave infrared HgCdTe avalanche photodiodes," J. Electron. Mater. **41**(10), 2928–2936 (2012).
26. B. E. A. Saleh, M. M. Hayat, and M. C. Teich, "Effect of dead space on the excess noise factor and time response of avalanche photodiodes," IEEE Trans. Electron Dev. **37**(9), 1976–1984 (1990).
27. J. D. Beck, R. Scritchfield, P. Mitra, W. W. Sullivan III, A. D. Gleckler, R. Strittmatter, and R. J. Martin, "Linear mode photon counting with the noiseless gain HgCdTe e-avalanche photodiode," Opt. Eng. **53**(8), 081905 (2014).
28. X. Sun, J. B. Abshire, J. D. Beck, P. Mitra, K. Reiff, and G. Yang, "HgCdTe avalanche photodiode detectors for airborne and spaceborne lidar at infrared wavelengths," Opt. Express **25**(14), 16589–16602 (2017).
29. Minamata Convention, "Minamata Convention on Mercury Text and Annexes" (Minamata Convention, 2017). http://www.mercuryconvention.org/. Accessed 27 April 2018.
30. S. Bhargava, H.-R. Blank, E. Hall, M. A. Chin, H. Kroemer, and V. Narayanamurti, "Staggered to straddling band lineups in InAs/Al(As, Sb)," Appl. Phys. Lett. **74**(8), 1135–1137 (1999).
31. P. J. Ker, J. P. R. David, and C. H. Tan, "Temperature dependence of gain and excess noise in InAs electron avalanche photodiodes," Opt. Express **20**(28), 29568–29576 (2012).
32. P. J. Ker, A. R. J. Marshall, A. B. Krysa, J. P. R. David, and C. H. Tan, "Temperature dependence of leakage current in InAs avalanche photodiodes," IEEE J. Quantum Electron. **47**(8), 1123–1128 (2011).